

# An approach to seismic inversion with quantum annealing

Sarah Greer<sup>\*1,2</sup> and Daniel O'Malley<sup>1</sup>

<sup>1</sup>Los Alamos National Laboratory; <sup>2</sup>Massachusetts Institute of Technology

## SUMMARY

Quantum computing has advanced enough that solving basic inverse problems in exploration seismology may be beneficial to show proof-of-concept results. The problems solved should be simple enough to work with the current early state of quantum computing hardware, which would be comparable to problems solved in the early stages of classical computing. We introduce an iterative algorithm for solving PDE-constrained optimization problems on a quantum annealer. We then use this method to invert for subsurface P-wave velocity—using a hybrid of classical and quantum computing—in a simple seismic experiment.

## INTRODUCTION

Over the past several years, research interest in applied fields utilizing quantum computing has increased with the arrival of more advanced hardware, such as the D-Wave 2000Q. Pioneering research utilizing early-stage quantum computing hardware may help establish the importance of quantum computing for the future of exploration geophysics.

Within the field of geophysics, Moradi et al. (2018) and Moradi et al. (2019) provide excellent overviews about the future of quantum computing in exploration seismology. Additionally, Sarkar and Levin (2018) looked at estimating material percentages from sparse offset-traveltime data using a quantum annealer.

While it may be early to leverage the power of quantum computing for practical, exploration-scale problems in geophysics, it is worth looking at simple applications to show proof-of-concept results. In this paper, we provide an early study of applying quantum computing to seismic inversion using Los Alamos National Laboratory's D-Wave 2000Q quantum annealer. For this study, we use a hybrid of classical and quantum computing. The inverse problem relies on a synthetic survey where geophones are placed at regular intervals on the surface over an area of interest. There is also a source placed on the surface at the center of the domain. We record the wavefield propagating from the source at the geophones and use these measurements to invert for subsurface P-wave velocity over the survey area, where our model is constrained such that each velocity mesh node can take one of two known values. We invert for the model iteratively, where each model update takes the form of a quadratic unconstrained binary optimization problem that can be solved by the quantum annealer.

## BACKGROUND

Quantum computing is a novel computational architecture with tremendous potential. The fundamental advantage of quantum computing over classical computing is the ability to encode information in *qubits* as opposed to the standard *bits* on a classical computer. While bits store logical data (either a 0 or a 1), qubits have the potential to hold a combination of these two states through quantum superposition. Quantum computers also benefit from quantum entanglement, where the state of one qubit affects the state of others. The combination of superposition and entanglement enables a quantum computer to, in some sense, store information that grows exponentially with the number of qubits. This exponential growth is in contrast to a classical computer where the information that can be stored grows linearly with the number of bits. All of this allows for a potentially significant speed-up in computation—sometimes an exponential speed-up (Shor, 1999; Harrow et al., 2009; Arute et al., 2019). However, there is a gap between these theoretical exponential speed-ups and practical problems, so the empirical study of the performance of quantum computers is currently of interest.

There are currently two hardware paradigms in quantum computing—universal gate-based computers and quantum annealing. While the universal gate-based approach is more versatile than quantum annealing, quantum annealers, like the D-Wave 2000Q that we use, have more qubits than gate-based hardware.

A call to the quantum annealer, in theory, returns the set of  $q_i$ s with the lowest energy in the form of

$$F_{\text{qubo}}(a_i, b_{i,j}; q_i) = \sum_i a_i q_i + \sum_j b_{i,j} q_i q_j, \quad (1)$$

where  $q_i \in \{0, 1\}$ , and  $a_i$  and  $b_{i,j}$  are weights specified by the problem. Minimizing this function is a quadratic unconstrained binary optimization (QUBO) problem, which the D-Wave 2000Q is designed to solve. Note that while the typical least-squares problem has an objective function that is always positive, QUBO objective functions can have negative values.

In practice, the quantum annealer typically only returns a near-optimal solution, and may not return the exact minimum. Because of this, the annealing process is performed multiple times to return an ensemble of  $q_i$ s that have the near-optimal energy. A more detailed overview of quantum annealing is Biswas et al. (2017).

Our goal is to develop an inversion strategy that utilizes the quantum annealer by formulating a problem that fits the form of a QUBO (equation 1).

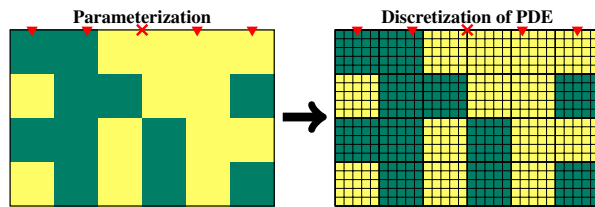


Figure 1: An example 2D continuous model space (left) is mapped to the discretization of the data space (right). Yellow represents low velocity ( $c_l$ ) and green represents high velocity ( $c_h$ ). The inverted red triangles represent receiver locations and the red X represents the location of the source with a co-located receiver.

## METHOD

In this seismic inversion experiment, our goal is to invert for subsurface P-wave velocity by propagating an acoustic wave through an unknown medium,  $\mathbf{c}$ , with the wavefield  $\mathbf{u}$  and source term  $\mathbf{s}$ , which can be modeled by

$$\left( \frac{1}{c^2} \frac{\partial^2}{\partial t^2} - \nabla \right) \mathbf{u} = \mathbf{s}. \quad (2)$$

We design a synthetic split-spread survey with sensors located on the surface at regular intervals and a source located at the center of the survey. The sensors measure the wavefield over time at those locations as the wave, originating at the source, propagates through the subsurface. We then use the measurements at the receivers to invert for the subsurface velocity model over the survey area, where our physical model is constrained such that each model mesh node can take one of two known velocity values. We denoted these two velocity values by  $c_h$  and  $c_l$  for the higher and lower velocity media, respectively. The reason we constrain our problem this way is for both physical and computational reasons. Physically, we could be inverting for the locations of two different geologic units. It also has a computational advantage—the quantum annealer solves binary optimization problems, so inverting for two values is a natural first step. We invert for the model iteratively, where each model update takes the form of a QUBO problem which the quantum annealer solves.

Our inversion strategy involves first defining a global objective function. This global objective function is what we ultimately want to minimize, and is not a QUBO. However, we also define separate objective functions to send to the quantum annealer during each iteration, and each of these is a QUBO approximation of the global objective function.

For the global objective function, we want to find the model that minimizes the  $\ell^2$ -norm of the residual between the observed and calculated wavefield values at the sensor locations. Additionally, for each iteration, we formulate the problem such that the model update is the solution of a QUBO that the quantum annealer can solve.

To demonstrate this process, we first generate a random model to set as truth—this is what we’re trying to invert for. We dis-

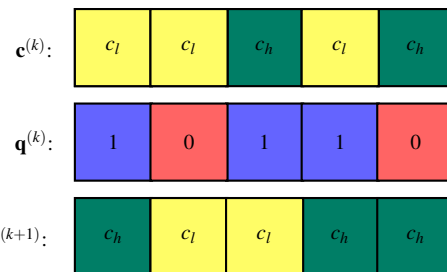


Figure 2: An example of how the qubits are flipped, as denoted by the  $\mathbf{B}$  operator, for  $\mathbf{c}, \mathbf{q} \in \{0, 1\}^5$  for iteration  $k + 1$ .

cretize the domain such that the computational mesh grid is finer than the discrete velocity changes in the physical domain, as seen in Figure 1. These two meshes allow us to solve for the physics accurately on the classical computer and solve an inverse problem that is small enough to fit on the quantum annealer. We then solve equation 2 using the true velocity model and store the values of the temporal evolution of the wavefield at the sensor locations. Using only these stored wavefield values at the sensor locations, called  $\hat{\mathbf{u}}$ , we want to invert for the true velocity model. To do that, we want to minimize the global objective function

$$\mathbf{F}_g(\mathbf{c}) = \sum_{n=1}^N |[\mathcal{U}(\mathbf{c})]_n - \hat{\mathbf{u}}_n|^2, \quad (3)$$

where  $\mathcal{U}$  is the fully non-linear forward modeling operator such that  $\mathcal{U}(\mathbf{c}) = \mathbf{u}$ ,  $\mathbf{c}$  is the velocity model,  $\hat{\mathbf{u}}$  is the measured wavefield, and  $n$  represents the index of the  $N$  different sensors that are measuring the wavefield. We attempt to minimize this global objective function using an iterative process, where each iteration involves solving a simpler optimization problem on the quantum annealer.

For any given iteration, we find the model update by creating a quadratic unconstrained binary optimization (QUBO) problem, which the quantum annealer can solve.

Our QUBO objective function,  $\mathbf{F}(\mathbf{q})$  is

$$\mathbf{F}(\mathbf{q}) = \sum_{n=1}^N |[\mathbf{U}(\mathbf{q})]_n - \hat{\mathbf{u}}_n|^2 \quad (4)$$

where  $\mathbf{U}(\mathbf{q})$  is a linear approximation of  $\mathcal{U}(\mathbf{c}) = \mathbf{u}$  such that

$$\mathbf{U}(\mathbf{q}) = \mathbf{u}_0 + \sum_{m=1}^M \mathbf{q}_m \mathbf{B}_m, \quad (5)$$

where  $\mathbf{B}_m$  is an operator which flips the bit at the  $m^{\text{th}}$  index then solves for the wavefield (equation 2),  $\mathbf{u}_0 = \mathcal{U}(\mathbf{c}_0)$ ,  $\mathbf{c}_0$  is the input velocity model, and  $\mathbf{q} \in \{0, 1\}^M$ . In  $\mathbf{c}$ , a value of 0 represents  $c_l$  and a value of 1 represents  $c_h$ , while in  $\mathbf{q}$  a value of 0 represents keeping the same bit for that index and a value of 1 represents flipping the bit for that index (Figure 2).

The least-squares objective function for iteration  $k$  is then equivalent to

$$\mathbf{F}^{(k)}(\mathbf{q}^{(k)}) = \|\mathbf{u}^{(k)} - \hat{\mathbf{u}}\|_2^2 + 2(\mathbf{u}^{(k)} - \hat{\mathbf{u}})^T \mathbf{B}^T \mathbf{q}^{(k)} + \mathbf{q}^{(k)T} \mathbf{B} \mathbf{B}^T \mathbf{q}^{(k)}. \quad (6)$$

After we've created the QUBO for this iteration, we send it (equation 6) to Los Alamos National Laboratory's D-Wave 2000Q quantum annealer which returns 10,000 possible solutions. We analyze the first several solutions that minimize the linearized objective function  $\mathbf{F}^{(i)}(\mathbf{q}^{(i)})$  (equation 6), and select the solution of those that minimizes the global objective function (3) and update the model accordingly. The selected solution is a  $\mathbf{q} \in \{0, 1\}^M$  vector which we use to update our model,  $\mathbf{k} \in \{0, 1\}^M$  as shown in Figure 2.

We then continue iterations until one of the following stopping criteria is met:

1.  $\mathbf{F}(\mathbf{c}) \leq \varepsilon$ , where  $\varepsilon$  is specified by the user. We chose  $\varepsilon = 0.03$ ;
2. the same solution is picked two iterations in a row; or
3. 10 iterations have passed.

We implement the method in Julia and use ThreeQ.jl, a Julia package that interfaces with D-Wave's quantum annealing hardware (O'Malley and Vesselinov, 2016).

## EXAMPLE

We apply this method to a  $0.8 \times 0.5$  kilometer domain where there are 8 possible velocity value locations in the horizontal direction and 5 possible velocity value locations in the vertical direction. We add 7 receivers spread over the surface of the domain where the source is a 35 Hz Ricker wavelet located at the center of the domain. The data are recorded for 400 milliseconds with a sampling rate of 0.001 seconds, and 10% Gaussian noise is added to the data.

We choose a random model to set as truth where the two units are chosen to represent sandstone, with  $c_h = 4750$  m/s, and shale, with  $c_l = 4250$  m/s. Figure 4a shows the true model and receiver layout. We choose an initial velocity model consisting entirely of  $c_h$ . Since there are  $8 \times 5 = 40$  possible locations for either  $c_l$  or  $c_h$  velocity values, there are  $2^{40} \approx 1.1 \times 10^{12}$  possible solutions. We run the experiment 25 times and analyze the results. The results of the 25 runs are shown in Figure 3. An example convergence pattern 3 is shown in Figure 4.

Generally, the method was able to produce a good velocity model and converged to the exact solution 8 out of the 25 model runs, or just under 1/3 of the time. 13 model runs concluded due to stopping criteria 1:  $\mathbf{F}(\mathbf{c}) \leq \varepsilon$ ; 11 model runs concluded due to stopping criteria 2: the same solution was picked two iterations in a row; and only one model run concluded due to stopping criteria 3: 10 iterations had passed. When there were errors in the resultant velocity model, they were typically located at maximum depth at the corners of the domain; the method was able to correctly invert for near-surface velocity well. This problem can be alleviated by adding more sources at different locations to the experiment. The method converged consistently within 10 iterations.

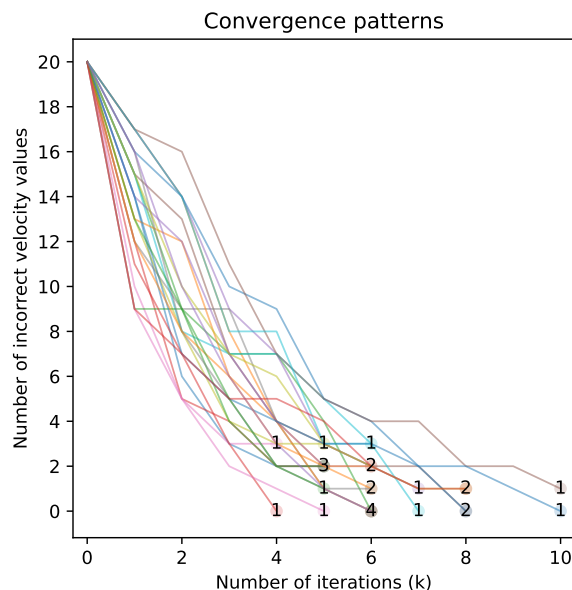


Figure 3: The number of incorrect velocity blocks (out of 40) versus the number of iterations for 25 different runs of the example problem discussed in this paper. Points represent where each model run stops, and numbers on the stopping points represent how many model runs converged with that number of iterations and incorrect velocity values.

## DISCUSSION

There are several distinct features about utilizing a quantum annealer to aid in inversion. First of all, the quantum annealer returns 10,000 possible solutions at every iteration, which are not usually all distinct. Of the distinct solutions, we look at the first 16 solutions with the lowest linearized objective function values, and of those pick the solution with the lowest non-linear objective function value. We look at multiple solutions, because the model that minimizes the linearized objective function may not be the same as the model that minimizes the non-linear objective function if the linear approximation isn't sufficiently accurate. The search for the best non-linear objective function among these 16 solutions can be performed in a perfectly parallel manner. There is a trade-off between having a better chance to find an optimal model update (which may require examining many possible solutions) and reducing the classical computational cost (which grows with the number of possible solutions examined). We found that examining the non-linear objective function value for 16 solutions resulted in a balance between these two objectives here. While not explored here, because the quantum annealer may return several near-optimal solutions, we could also use the distribution of solutions returned to aid in uncertainty quantification.

Secondly, the quantum annealer behaves stochastically, so the samples returned for a given QUBO problem is random (approximately following a Boltzmann distribution). That is why running the same problem with the same truth and starting models multiple times can have different convergence behavior.

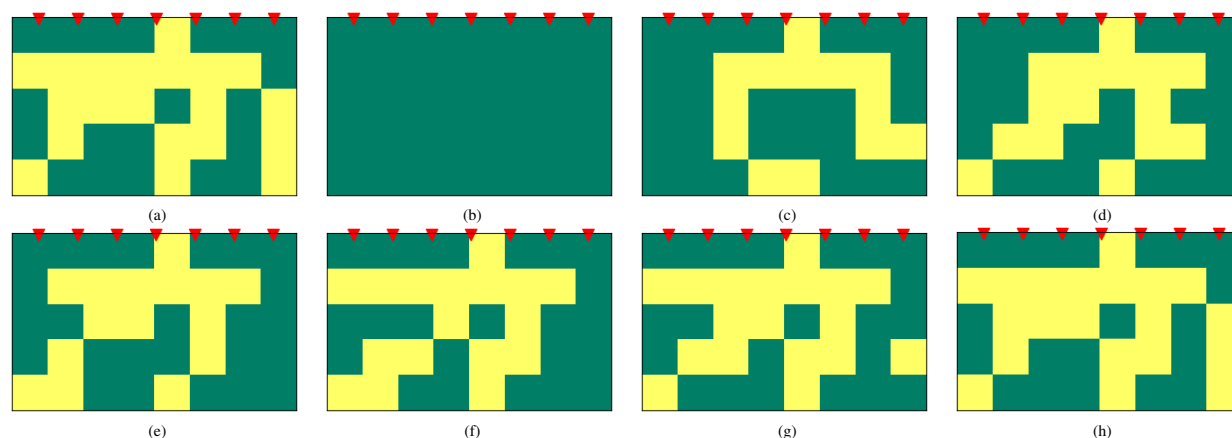


Figure 4: An example convergence pattern from the example model. (a) truth; (b) initial model; (c) first iteration; (d) second iteration; (e) third iteration; (f) fourth iteration; (g) fifth iteration; (h) sixth iteration.

ior.

Finally, the difference between  $c_l$  and  $c_h$  may affect the success of the method. While having a large impedance contrast between units makes the linear approximation worse, it also affects the solution output by the quantum annealer as the governing QUBO may have coefficients that are lower than the quantum annealer's hardware **noise floor**. A current topic of research is trying to alleviate this problem by utilizing **classical pre- and post-processing** (Golden and O'Malley, 2019).

There are also two technical distinctions for terminology used in this quantum computing application. There is a notable difference between **logical qubits and physical qubits**. When we refer to qubits in our problem description, we are referring to logical qubits. However, when the problem is sent to the quantum annealer, these logical qubits must be mapped to the physical qubits present on the quantum annealer. In the Chimera graph that is used by the D-Wave 2000Q quantum annealer, each physical qubit can be coupled with up to six other physical qubits. However, the problems that we send to the quantum annealer generally require each logical qubit to be coupled with more than six other qubits. When the logical qubits are mapped to physical qubits, each logical qubit consists of multiple physical qubits. These physical qubits act together to return one solution, and their combined connectivity makes it so the corresponding logical qubit can be coupled with the necessary logical qubits. **This mapping of logical qubits to multiple qubits is called embedding**. Although the problem uses 40 logical qubits, the embedding uses 688 physical qubits out of the available 2034 physical qubits. LANL's D-Wave 2000Q comes with 2048 physical qubits, but 14 physical qubits are inoperable due to hardware imperfections.

Another technical distinction is that the term "quantum annealing" has also been used in exploration geophysics applications as a type of global optimization algorithm to avoid converging to local minima, as in Alulawi and Sen (2015) and Zhao et al. (2016). The semantics of this terminology is distinctly different from the quantum annealing described in this paper.

Additional work in this field might utilize the fact that the wave equation can be formulated as a polynomial or monomial of degree 2, or expand upon the finite difference approximation as is done in O'Malley (2018). Furthermore, this work could be expanded to more than two units, e.g., by using a one-hot encoding or may further look at uncertainty quantification from the distribution of returned solutions from the quantum annealer.

It is inevitable that as quantum computing hardware improvements occur over the next several years, scientists in applied fields will increasingly achieve better results as algorithmic developments are subsequently made. With parallel progress in both hardware and algorithmic development, we hope to eventually surpass classical performance for problems in fields such as exploration geophysics.

## CONCLUSIONS

In this paper, we provide a first attempt at inverting for P-wave velocity in a simple seismic experiment using a new computational architecture—quantum annealing. We applied our method to a simple synthetic split-spread seismic survey by introducing an iterative method to solve for velocity using surface geophone measurements. We ran this experiment 25 times, and the results were promising: the method was successfully able to recover the model perfectly about 1/3 of the time.

## ACKNOWLEDGEMENTS

We would like to acknowledge John Golden for useful discussions. Sarah Greer acknowledges support from the United States Department of Energy through the Computational Science Graduate Fellowship (DOE CSGF) under grant number DE-SC0019323. Daniel O'Malley acknowledges support from the National Nuclear Security Administration's Advanced Simulation and Computing program.

## REFERENCES

- Alulawi, B., and M. K. Sen, 2015, Prestack seismic inversion by quantum annealing: Application to Cana field: 85th Annual International Meeting, SEG, Expanded Abstracts, 3507–3511, doi: <https://doi.org/10.1190/segam2015-5831164.1>.
- Arute, F., K. Arya, R. Babbush, D. Bacon, J. C. Bardin, R. Barends, R. Biswas, S. Boixo, F. G. Brandao, D. A. Buell, B. Burkett, Y. Chen, Z. Chen, B. Chiaro, R. Collins, W. Courtney, A. Dunsworth, E. Farhi, B. Foxen, A. Fowler, C. Gidney, M. Giustina, R. Graff, K. Guerin, S. Habegger, M. P. Harrigan, M. J. Hartmann, A. Ho, M. Hoffmann, T. Huang, T. S. Humble, S. V. Isakov, E. Jeffrey, Z. Jiang, D. Kafri, K. Kechedzhi, J. Kelly, P. V. Klimov, S. Knysh, A. Korotkov, F. Kostritsa, D. Landhuis, M. Lindmark, E. Lucero, D. Lyakh, S. Mandrà, J. R. McClean, M. McEwen, A. Megrant, X. Mi, K. Michielsen, M. Mohseni, J. Mutus, O. Naaman, M. Neeley, C. Neill, M. Y. Niu, E. Ostby, A. Petukhov, J. C. Platt, C. Quintana, E. G. Rieffel, P. Roushan, N. C. Rubin, D. Sank, K. J. Satzinger, V. Smelyanskiy, K. J. Sung, M. D. Trevithick, A. Vainsencher, B. Villalonga, T. White, Z. J. Yao, P. Yeh, A. Zalcman, H. Neven, and J. M. Martinis, 2019, Quantum supremacy using a programmable superconducting processor: *Nature*, **574**, 505–510, doi: <https://doi.org/10.1038/s41586-019-1666-5>.
- Biswas, R., Z. Jiang, K. Kechedzhi, S. Knysh, S. Mandrà, B. O’Gorman, A. Perdomo-Ortiz, A. Petukhov, J. Realpe-Gómez, E. Rieffel, D. Venturelli, F. Vasko, and Z. Wang, 2017, A NASA perspective on quantum computing: Opportunities and challenges: *Parallel Computing*, **64**, 81–98.
- Golden, J. K., and D. O’Malley, 2019, Pre-and post-processing in quantum-computational hydrologic inverse analysis: arXiv preprint arXiv:1910.00626.
- Harrow, A. W., A. Hassidim, and S. Lloyd, 2009, Quantum algorithm for linear systems of equations: *Physical Review Letters*, **103**, 150502, doi: <https://doi.org/10.1103/PhysRevLett.103.150502>.
- Moradi, S., D. Trad, and K. A. Innanen, 2018, Quantum computing in geophysics: Algorithms, computational costs, and future applications: 88th Annual International Meeting, SEG, Expanded Abstracts, 4649–4653, doi: <https://doi.org/10.1190/segam2018-2998507.1>.
- Moradi, S., D. Trad, and K. A. Innanen, 2019, When quantum computers arrive on seismology’s doorstep: **44**, 1–20.
- O’Malley, D., 2018, An approach to quantum-computational hydrologic inverse analysis: *Scientific Reports*, **8**, 1–9.
- O’Malley, D., and V. V. Vesselinov, 2016, ToQ.jl: A high-level programming language for D-Wave machines based on Julia: 2016 IEEE High Performance Extreme Computing Conference (HPEC), IEEE, 1–7.
- Sarkar, R., and S. A. Levin, 2018, Snell tomography for net-to-gross estimation using quantum annealing: 88th Annual International Meeting, SEG, Expanded Abstracts, 5078–5082, doi: <https://doi.org/10.1190/segam2018-2998409.1>.
- Shor, P. W., 1999, Polynomial-time algorithms for prime factorization and discrete logarithms on a quantum computer: *SIAM Review*, **41**, 303–332, doi: <https://doi.org/10.1137/S0036144598347011>.
- Zhao, C., G. Zhang, and L. Lu, 2016, The stochastic inversion based on QA algorithm and FFT-MA simulation: SPG/SEG 2016 International Geophysical Conference, 524–526.

**This article has been cited by:**

1. Marcin Dukalski, Diego Rovetta, Stan van der Linde, Matthias Möller, Niels Neumann, Frank Phillipson. 2023. Quantum computer-assisted global optimization in geophysics illustrated with stack-power maximization for refraction residual statics estimation. *GEOPHYSICS* **88**:2, V75-V91. [[Abstract](#)] [[Full Text](#)] [[PDF](#)] [[PDF w/Links](#)]
2. Shogo Masaya, Shuichi Desaki. 2022. 3D seismic data processing using cloud computing. *Journal of the Japanese Association for Petroleum Technology* **87**:1, 45-50. [[Crossref](#)]